

Effect of C/Ti ratio on the compressive properties and wear properties of the 50 vol.-% submicron-sized TiC_x /2014Al composites fabricated by combustion synthesis and hot press consolidation

F. Qiu, Y.-Y. Gao, J.-Y. Liu, S.-L. Shu, Q. Zou, T.-Z. Zhang & Q.-C. Jiang

To cite this article: F. Qiu, Y.-Y. Gao, J.-Y. Liu, S.-L. Shu, Q. Zou, T.-Z. Zhang & Q.-C. Jiang (2016) Effect of C/Ti ratio on the compressive properties and wear properties of the 50 vol.-% submicron-sized TiC_x /2014Al composites fabricated by combustion synthesis and hot press consolidation, Powder Metallurgy, 59:4, 256-261, DOI: [10.1080/00325899.2016.1172829](https://doi.org/10.1080/00325899.2016.1172829)

To link to this article: <http://dx.doi.org/10.1080/00325899.2016.1172829>



Published online: 13 May 2016.



Submit your article to this journal [↗](#)



Article views: 107



View related articles [↗](#)



View Crossmark data [↗](#)



Citing articles: 1 View citing articles [↗](#)

Effect of C/Ti ratio on the compressive properties and wear properties of the 50 vol.-% submicron-sized TiC_x/2014Al composites fabricated by combustion synthesis and hot press consolidation

F. Qiu^{1,3}, Y.-Y. Gao¹, J.-Y. Liu¹, S.-L. Shu², Q. Zou³, T.-Z. Zhang¹ and Q.-C. Jiang^{*1}

In this study, *in situ* 50 vol.-% TiC_x/2014Al composites with different C/Ti molar ratios (0.6, 0.7, 0.8, 0.9 and 1) were successfully produced by the method of combustion synthesis and hot press consolidation. The microstructure and the mechanical properties of the composites were investigated. Microstructure characterisation of the TiC_x/2014Al composites showed relatively uniform distribution of the TiC_x particles with the particle size in the range of 200–900 nm. With the increase of the C/Ti molar ratio, the yield strength ($\sigma_{0.2}$) and the ultimate compression strength (σ_{UCS}) increased first then decreased, and the fracture strain (ϵ_f) increased. The $\sigma_{0.2}$, σ_{UCS} and the abrasive wear resistance of the 50 vol.-% TiC_x/2014Al composites reached the highest value when the value of the C/Ti molar ratio comes to 0.8. The $\sigma_{0.2}$, σ_{UCS} and ϵ_f of the 50 vol.-% TiC_x/2014Al composites with the C/Ti molar ratio of 0.8 are 1094 MPa, 1454 and 6.13%, respectively.

Keywords: Aluminium matrix composites, Structural materials, Mechanical properties, Microstructure

Introduction

The aluminium matrix composites reinforced with TiC ceramic particles have been extensively researched.^{1–4} As a good reinforcement phase in aluminium matrix composites, TiC ceramic particles exhibit many good features, such as high elastic modulus, high hardness, low thermal expansion coefficient, good thermodynamic stability and preferable wettability with molten aluminium.^{1–5} As a type of advanced engineering material, the composites reinforced with TiC ceramic particles possess not only the advantages of metal materials (ductility and toughness) but also the characteristics of ceramic materials (high strength and elastic modulus). Hence, the composites reinforced with TiC ceramic particles exhibit good mechanical properties. The preparation of composites mainly include the traditional casting method and the *in situ* method. The proliferation of the *in situ* method used for preparing metal matrix composites is due to

many factors, such as good interface between the reinforcement phase and matrix, pure reaction products with small ceramic size and stable properties.^{6–11}

Shu *et al.*³ investigated the compressive behaviours and abrasive wear resistance of the 50, 60 and 70 vol.-% TiC_x/Al composites, which were prepared by the *in situ* method of combustion synthesis and hot press consolidation. The compressive strength of the three composites were 714, 815 and 744 MPa, respectively. The relatively higher strength of the TiC_x/Al composites could be attributed to the selection of ceramic particles and the *in situ* fabrication method. Xuan *et al.*¹² performed compression tests with 50 vol.-% TiC_x/Al and 50 vol.-% TiB₂/Al composites in the strain rate range from $1 \times 10^{-4} \text{ s}^{-1}$ to $1 \times 10^{-1} \text{ s}^{-1}$. Meanwhile, they investigated the effect of strain rate on the compressive behaviours and the work-hardening capacity of the composites. The σ_{UCS} of the 50 vol.-% TiC_x/Al and the 50 vol.-% TiB₂/Al composites are 615 and 1071 MPa when the strain rate is $1 \times 10^{-4} \text{ s}^{-1}$. Yang *et al.*¹³ produced the *in situ* TiC/Al composite by an innovative spray-deposition technique. They found that the needle-like Al₃Ti, which is detrimental to the fracture toughness and the stability of the microstructure, could be eliminated completely from the final product by using a proper Ti/C molar ratio of 1:1.3 in the Ti–C–Al performs. Birol¹⁴ produced the experimental Al–3Ti–0.75C alloy in the Marmara Research Center. Al–10Ti melt was first diluted to a Ti level of 3% and then treated

¹Key Laboratory of Automobile Materials, Ministry of Education, Department of Materials Science and Engineering, Jilin University, No. 5988 Renmin Street, 130025 Changchun, China

²State Key Laboratory of Luminescence and Applications, Changchun Institute of Optics, Fine Mechanics and Physics, Chinese Academy of Sciences, 130012 Changchun, China

³Department of Mechanical Engineering, Oakland University, Rochester, MI 48309, US

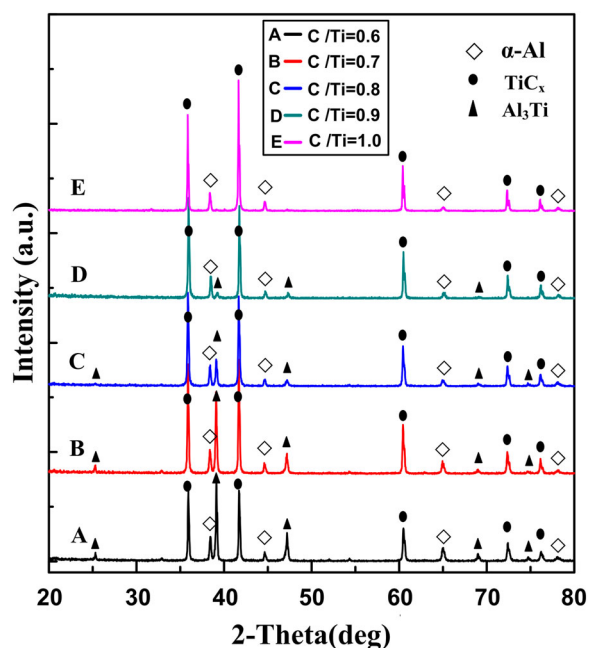
*Corresponding author, email jqc@jlu.edu.cn

with a specially designed graphite rotor to establish a chemical reaction between the titanium dissolved in molten aluminium and solid carbon at the surface of the graphite rotor. They revealed that the grain refinement performance was improved notably when extra Ti on top of the TiC stoichiometry was made available in the aluminium melt. Jin *et al.*^{15,16} indicated that the stoichiometry had great effects on the properties of the atomic bond in different crystal orientations, and the TiC_x stoichiometry played an important role in its growth process. It was found that the TiC_x (0.47 < x < 0.98) changed its growth shapes by varying stoichiometry during the combustion synthesis in an Al-Ti-C system, i.e. with the increase of the stoichiometry (x) of TiC_x, the TiC_x particles turned their growth shapes from octahedron to sphere.^{15,16} Thus, C/Ti molar ratios in Al-Ti-C system are important for the preparation of TiC_x/2014Al composites. Up to now, the investigation of the effect of the C/Ti molar ratio on the compressive behaviour and abrasive wear resistance of TiC_x/Al composites has not been reported.

In the present paper, the 50 vol.-% TiC_x/2014Al composites with different C/Ti molar ratios (0.6, 0.7, 0.8, 0.9 and 1) were produced by the *in situ* method of combustion synthesis and hot press consolidation. In addition, the effect of the C/Ti molar ratio on the microstructure, compression behaviour and abrasive wear properties of the composites were investigated in detail.

Sample preparation and testing

The base material was made of commercial powders of 2014Al (99% purity, ~47 μm), titanium (99.5% purity, ~25 μm) and carbon black (99.9% purity). Carbon black and titanium, with molar ratios of 0.6, 0.7, 0.8, 0.9 and 1, respectively, and nominal composition of 50 vol.-%/2014Al, were used for the powder blend. The



1 XRD patterns of the 50 vol.-% TiC_x/2014Al composites with different C/Ti molar ratios a C/Ti = 0.6, b C/Ti = 0.7, c C/Ti = 0.8, d C/Ti = 0.9, e C/Ti = 1

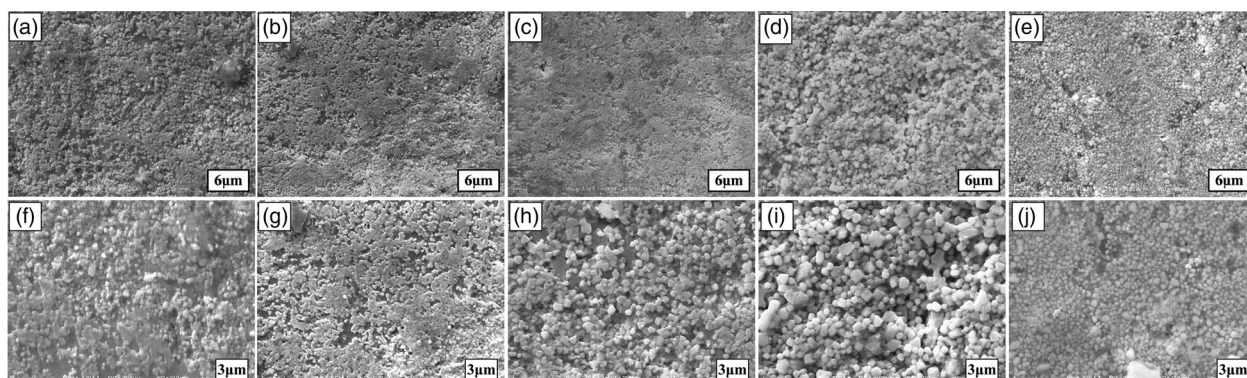
compositions of 2014Al were given in Table 1. The powders were mixed sufficiently by ball milling for 20 h and then cold pressed into a cylindrical form using a stainless steel die. The powder briquetting sample, with 29 mm in diameter, approximately 38 mm in height, and green density of approximately 65 ± 2% theoretical density, was put in a graphite mould. After that the mould was placed into a vacuum thermal explosion furnace and heated in a vacuum atmosphere. The heating rate of the furnace was about 30 K min⁻¹ and the temperature at the centre of the briquetting was measured by Ni-Cr/Ni-Si thermocouples. When the temperature suddenly jumped up, indicating that the sample should be ignited, the sample was quickly pressed just when it was still hot and soft under the pressure of 40 MPa. The pressure was kept constant for 20 s and then the sample was cooled down to the room temperature.

The phase constituent of the samples was investigated by X-ray diffraction (XRD, Moldel D/Max 2500PC Rigaku, Japan) with Cu Kα radiation. The microstructure was investigated by a scanning electron microscopy (SEM, Moldel Evo18 Carl Zeiss, Germany). To clearly observe the morphology of the synthesised ceramic particles in the composites, a fragment of the composites was immersed in an 18 vol.-% HCl to remove the Al coating on the surface of the ceramic particles. The size and shape of the extracted ceramic particles were observed using a field emission scanning electron microscope (FESEM, JSM6700F, Japan). The cylindrical specimens with a diameter of 3 mm and a length of 6 mm were used for the compression tests. The loading surfaces were polished to make sure they were parallel to each other. Uniaxial compression tests were carried out using a servo-hydraulic material testing system (MTS 810, USA) with a strain rate of 1 × 10⁻⁴ s⁻¹. Microhardness of the composites was measured by a Vickers hardness tester (1600-5122VD Micromet 5104, USA) with a static load of 10 N and a dwell time of 15 s. The average hardness value was determined based on 10 indentations. The elastic modulus tests were detected by an ultrasonic etching thickness gauge (Olympus-NDT, 38DLP-XT).

Abrasive wear tests were carried out with a pin-on-disk apparatus at the room temperature. The composites were machined into the pin samples with dimensions of 4 × 4 × 15 mm, and the 4 × 4 mm face was employed as the wear surface. Al₂O₃ abrasive paper with abrasive particle size of ~20 μm (600 grit) was used as the disk sample. The rotation speed of the disk was 60 rev min⁻¹, the applied normal loads were 15, 25 and 35 N, the wear track diameter is 210 mm, and the sliding distance was kept constant at 24.78 m. The worn Al₂O₃ abrasive paper was replaced for every sliding distance of 8.26 m, making sure that the samples would contact with the fresh abrasive particles. The abrasive wear rate of the composites was defined as the volume loss per unit sliding distance, and the volume loss is obtained from the ratio of weight loss to the density of the composites. The weight loss was obtained by measuring the pin sample before and after the wear test using an electronic balance with a resolution of 0.1 mg. The density of the composite was measured by Archimedes' water-immersion method. Each test was repeated for three times and the average of the three tests was calculated. The worn surfaces and the pullout of the TiC_x/2014Al composites with different C/Ti molar ratios were examined by SEM.

Table 1 Chemical compositions of the cast hypereutectic 2014 alloy (wt-%)

Al	Si	Cu	Mg	Zn	Mn	Ti	Ni	Fe
Bal	0.6–1.6	3.9–4.8	0.4–0.8	≤0.3	0.4–1.0	≤0.15	≤0.10	0.0–0.7

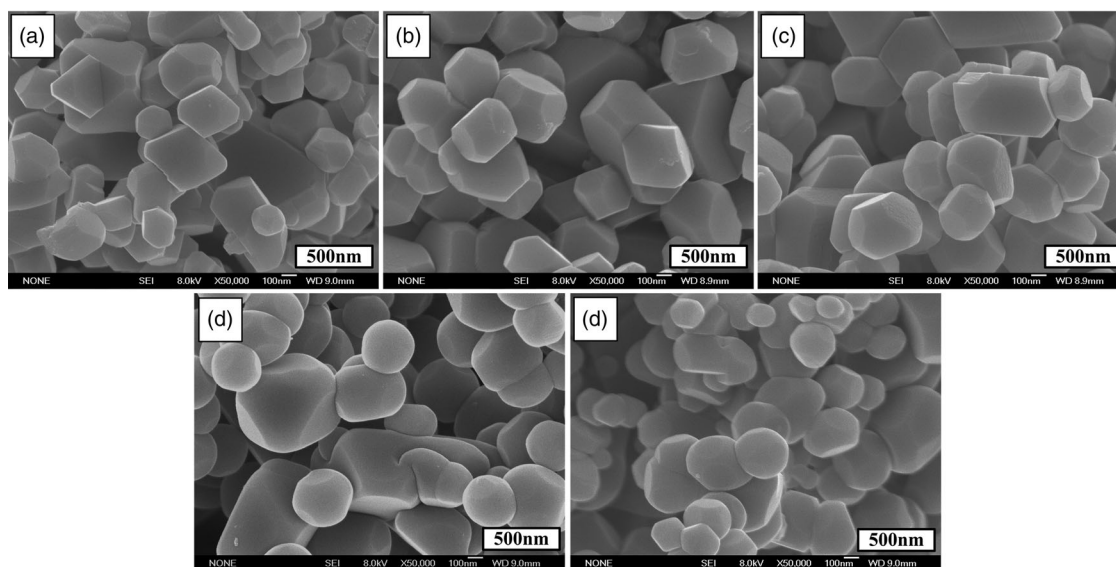


2 SEM images of the 50 vol.-% $TiC_x/2014Al$ composites with different C/Ti molar ratios a C/Ti = 0.6, b C/Ti = 0.7, c C/Ti = 0.8, d C/Ti = 0.9, e C/Ti = 1, the figures f–j are corresponding to the high magnification view in the figures a–e, respectively

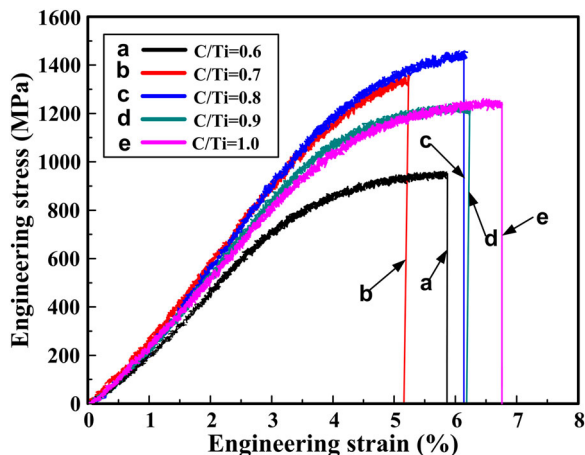
Results and discussion

The X-ray diffraction results of the 50 vol.-% $TiC_x/2014Al$ composites with different C/Ti molar ratios are shown in Fig. 1. It can be seen that the products in the samples are mainly TiC_x and $\alpha-Al$ phases. Meanwhile, some Al_3Ti phases exist in the samples when the C/Ti molar ratio equal to 0.6, 0.7, 0.8 and 0.9. The intensity of the Al_3Ti peaks decreases with the increase of the C/Ti molar ratio. Figure 2a–e shows the SEM images of etched surfaces of the 50 vol.-% $TiC_x/2014Al$ composites with different C/Ti molar ratios. Figure 2f–j is the high magnification view of Fig. 2a–e, correspondingly. In Fig. 2f–j, the synthesised TiC_x particles in the $TiC_x/2014Al$ composites exhibit a uniform distribution in the aluminium matrix. The pictures in Fig. 3 show the magnification of the TiC_x particles extracted from the 2014Al

matrix with 18 vol.-% HCl-distilled water solution. As indicated, the size of the TiC_x particles formed in these $TiC_x/2014Al$ composites is in the range of 200–900 nm. Moreover, the TiC_x particles evolve from octahedron to truncated octahedron and finally to close-to-sphere with the C/Ti molar ratio increasing to 1. The TiC_x , non-stoichiometric composition was determined by lattice parameter measurement using X-ray diffraction analysis. We discussed five angle ranges (35–37, 40–43, 59.5–61, 71.5–73 and 75–77) of the TiC_x phase in the 50 vol.-% $TiC_x/2014Al$ composites with different C/Ti molar ratios. The lattice constant was calculated through the surface spacing of the TiC_x phase with different C/Ti molar ratios. Finally, the actual values of stoichiometry (x) of TiC_x were confirmed by curve fitting the lattice constant and the C/Ti molar ratio. The calculated result shows that the values of x for the TiC_x phase were 0.67, 0.69,



3 FESEM images of the ceramic particles extracted from the 50 vol.-% $TiC_x/2014Al$ composites with different C/Ti molar ratios a C/Ti = 0.6, b C/Ti = 0.7, c C/Ti = 0.8, d C/Ti = 0.9 and e C/Ti = 1



4 Compression engineering stress–strain curves of the 50 vol.-% $TiC_x/2014Al$ composites with different C/Ti molar ratios a C/Ti=0.6, b C/Ti=0.7, c C/Ti=0.8, d C/Ti=0.9 and e C/Ti=1

0.70, 0.72 and 0.97 with different C/Ti molar ratios of 0.6, 0.7, 0.8, 0.9 and 1.0, respectively. The value of x increases with the increase of the C/Ti molar ratio.

Figure 4 shows the compressive engineering stress–strain curves of the 50 vol.-% $TiC_x/2014Al$ composites with different C/Ti molar ratios. The compression properties and relative density of the $TiC_x/2014Al$ composites are summarised in Table 2. It can be seen that the $\sigma_{0.2}$ and σ_{UCS} increase first then decrease with the increase of C/Ti molar ratio from 0.6 to 1. Frumin *et al.*¹⁷ hold the opinion that, the lower the value of x in TiC_x , the more dominant the metallic character of the bonding in the compound will be, leading to the enhancement of the chemical interaction with Al (L). Therefore, lowering the value of x can improve the mechanical properties of TiC_x/Al composites. The value of x increases with the increase of the C/Ti molar ratio. So, the mechanical properties of TiC_x/Al composites would be improved with the decrease of the C/Ti molar ratio from 1.0 to 0.6. Meanwhile, the intensity of the Al_3Ti peaks decreases with the increase of the C/Ti molar ratio. The presence of this phase is undesirable because it is a brittle phase. The two kinds of influence mechanism have a competitive relationship. Eventually, the 50 vol.-% $TiC_x/2014Al$ composites with the C/Ti molar ratio of 0.8 get the best compression performance.

Figure 5a–e shows SEM images of the compression fracture surfaces of the 50 vol.-% $TiC_x/2014Al$ composites with different C/Ti molar ratios. Compared to the octahedral TiC particles, the spherical ceramic particles could largely reduce the stress concentration and the formation of cracks.^{18,19} And the content of the Al_3Ti phase decreases with the increase in the C/Ti molar ratios. Too

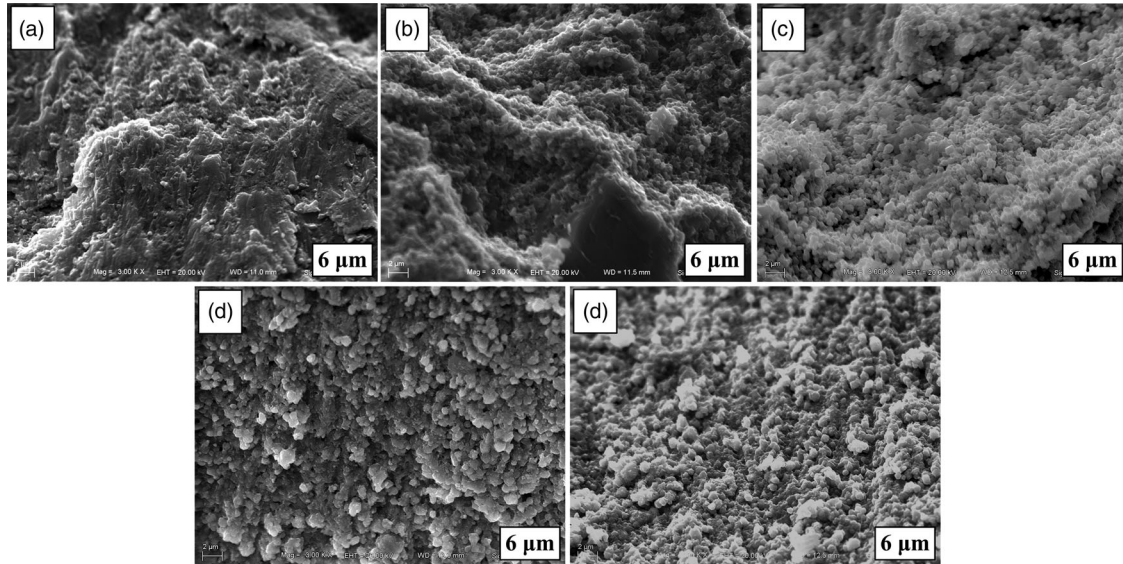
much Al_3Ti brittle phase would reduce the fracture toughness of the $TiC_x/2014Al$ composites. Therefore, the ϵ_f of the $TiC_x/2014Al$ composites increases with the increase of the C/Ti molar ratio.

Figure 6 shows the variation of the wear rate with the applied load (15, 25 and 35 N) for the $TiC_x/2014Al$ composites tested under the Al_2O_3 abrasive particles with the size of 20 μm . It can be seen that the abrasive wear resistance and the hardness of the $TiC_x/2014Al$ composites increase first then decrease with the increase of C/Ti molar ratio from 0.6 to 1. It is apparent that the $TiC_x/2014Al$ composite with C/Ti molar ratio of 0.8 experience an extremely low wear rate. It is found that the $TiC_x/2014Al$ composite with the C/Ti molar ratio of 0.8 has the highest hardness as shown in Table 2. The Al_2O_3 abrasives cannot penetrate easily into the harder composite during sliding, resulting in little material removal from the surface. This can also be confirmed by the worn surfaces of the $TiC_x/2014Al$ composites tested under the load of 25 N and the Al_2O_3 abrasive particle size of 20 μm , shown in Fig. 7a–d. All the worn surfaces show scratches formed by plastic deformation, with evidence of material removal by cutting and ploughing. The worn surface of the 50 vol.-% $TiC_x/2014Al$ composite with the C/Ti molar ratio of 0.8 shown in Fig. 7c is much smoother than other $TiC_x/2014Al$ composites shown in Fig. 7a, b, d and e. According to these results, we presume that the hard TiC_x particles in the composites can act as a barrier to reduce the cutting efficiency of the Al_2O_3 abrasive particles and the plastic deformation of aluminium matrix during wear. The $TiC_x/2014Al$ composite with the C/Ti molar ratio of 0.8, with the highest hardness, highest relative density and best compression performance, will generate stronger resistance to the Al_2O_3 abrasive particles and highest abrasive wear resistance. Thus, the 50 vol.-% $TiC_x/2014Al$ composite with C/Ti molar ratio of 0.8 possesses the relatively best wear resistance. Meanwhile, the TiC_x ceramic particles with sharp edges and corners in 50 vol.-% $TiC_x/2014Al$ composites with the C/Ti molar ratios of 0.6 and 0.7 would result in stress concentration, hence the TiC_x particles are easier to fall from the aluminium matrix and the worn surfaces of the above two kinds of composites are much rougher.

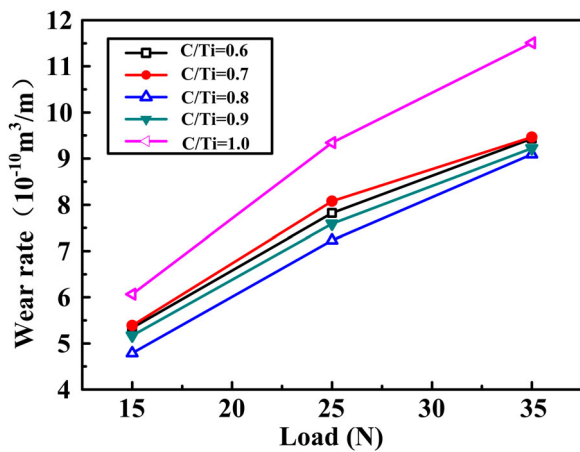
It can also be seen from Fig. 6 that the wear rate of the composites increases with the increase in the load. The Al_2O_3 abrasives will penetrate deeper as the applied load increases and subsequently result in high wear rate.²⁰ When the applied load is relatively large (applied load of 35 N), the TiC_x ceramic particles are easily escaped from the aluminium matrix. Thus, the abrasive wear resistance of the $TiC_x/2014Al$ composites decreases significantly when the applied load is relatively large. Meanwhile, when the applied load changes in the range of 15–35 N, the 50 vol.-% $TiC_x/2014Al$ composite with

Table 2 Compression properties and relative density of the $TiC_x/2014Al$ composites

Composites	Relative density (%)	$\sigma_{0.2}$ (MPa)	σ_{UCS} (MPa)	ϵ_f (%)	Hv	E (GPa)
C/Ti = 0.6	96.6 ± 0.2	555 ± 12	928 ± 19	5.85 ± 0.23	310.5 ± 5.3	196 ± 2
C/Ti = 0.7	96.9 ± 0.2	1023 ± 23	1342 ± 33	5.23 ± 0.19	308.7 ± 3.9	211 ± 2
C/Ti = 0.8	97.1 ± 0.3	1094 ± 27	1454 ± 45	6.13 ± 0.25	326.6 ± 6.5	211 ± 3
C/Ti = 0.9	96.3 ± 0.2	832 ± 22	1211 ± 26	6.20 ± 0.27	317.3 ± 2.8	194 ± 2
C/Ti = 1.0	96.1 ± 0.2	894 ± 25	1215 ± 28	6.75 ± 0.26	289.5 ± 3.4	197 ± 3



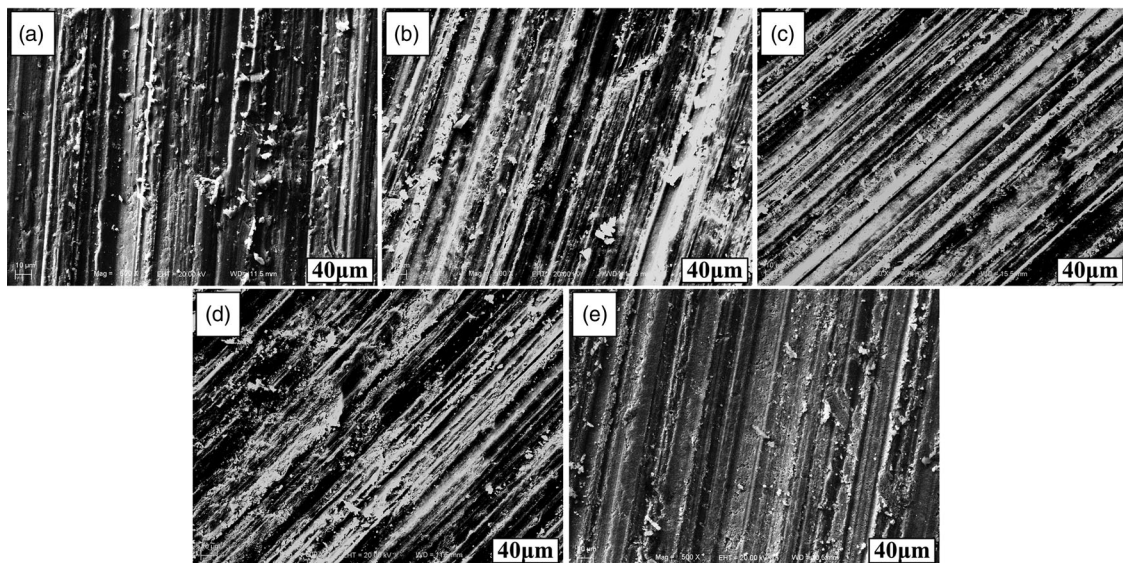
5 SEM images of the compression fracture surfaces of the 50 vol.-% $TiC_x/2014Al$ composites with different C/Ti molar ratios a C/Ti = 0.6, b C/Ti = 0.7, c C/Ti = 0.8, d C/Ti = 0.9, e C/Ti = 1



6 Wear rate vs. applied load tested under Al_2O_3 abrasive particle size of $20 \mu m$ for the 50 vol.-% $TiC_x/2014Al$ composites with different C/Ti molar ratios

C/Ti molar ratio of 0.8 processes the relatively better abrasive wear resistance.

As mentioned above, the abrasive wear behaviour of the $TiC_x/2014Al$ composites consists of two steps.²¹ First, the Al_2O_3 abrasive particles penetrate into the soft aluminium matrix and cut it, resulting in excessive aluminium fragment removal from the composites. At the same time, the TiC_x particles can act as obstacles to the impact of the Al_2O_3 abrasive particles. The interactions between the TiC_x particles and the Al_2O_3 abrasive particles lead to the blunting of the Al_2O_3 abrasive particles. Second, when the TiC_x particles are loosened and sheared out from the aluminium matrix during the wear test, the TiC_x particles in the subsurface will present on the worn surface, and they protect the softer aluminium matrix again during the following wear test. The TiC_x ceramic particles expose from the aluminium matrix and tact as a barrier to the micro-cutting action of the abrasives, inducing the decrease in the cutting efficiency of the



7 Worn surfaces of the 50 vol.-% $TiC_x/2014Al$ composites with different C/Ti molar ratio tested under the applied load of 25 N and the Al_2O_3 abrasive particle size of $20 \mu m$. a C/Ti = 0.6, b C/Ti = 0.7, c C/Ti = 0.8, d C/Ti = 0.9, e C/Ti = 1

Al₂O₃ abrasives and the wear rate of the composites. When the exposed TiC_x ceramic particles escape from the worn surface of the composites, the Al₂O₃ abrasives will impact the aluminium matrix and the TiC_x ceramic particles simultaneously again. The abrasive wear behaviour of the TiC_x/2014Al composites can be concluded as that the Al₂O₃ abrasive particles cut the ductile aluminium matrix and impact the TiC_x particles simultaneously.

Conclusions

The 50 vol.-% TiC_x/2014Al composites with different C/Ti molar ratios were successfully fabricated by the *in situ* method of combustion synthesis and hot press consolidation. With the increase of the C/Ti molar ratio, the shape of the *in situ* TiC_x ceramic particles changes from octahedral to spherical or near spherical, the yield strength, maximum compressive strength and elastic modulus of the TiC_x/2014Al composites increase first then decrease, and the compressive fracture strain increases. The *x* value of the TiC_x decreases with the decrease in the C/Ti molar ratios, the metallicity of the TiC_x particles increases, the wettability between TiC_x particles and the Al matrix is improved; Meanwhile, the content of the Al₃Ti brittle phase in the composites increases with the decrease of the C/Ti molar ratio. The stress concentration existing in the surface edges of the octahedral TiC_x ceramic particles leads to crack initiation and the reduction of the material compression performance. It is optimised that the 50 vol.-% TiC_x/2014Al composite with the C/Ti molar ratio of 0.8 has the best compression performance and wear resistance. Its hardness, yield strength, maximum compression strength, fracture strain and elastic modulus are 326.6 HV, 1094 MPa, 1454 MPa, 6.13% and 211 GPa, respectively.

Acknowledgements

This work is supported by the National Natural Science Foundation of China (NNSFC, No. 51571101), National Basic Research Program of China (973 Program, No. 2012CB619600), NNSFC (No. 51171071 and No. 51501176), the 'twelfth five-year plan' Science & Technology Research Foundation of Education Bureau of Jilin Province, China (Grant No. 2015-479), the State Scholarship Fund of China Scholarship Council (No. 201506175140), the Innovation Experimental Training Project of Jilin University in 2015 (No. 2015430457) and the Project 985-High Properties Materials of Jilin University.

References

1. S. L. Shu, J. B. Lu, F. Qiu, Q. Q. Xuan and Q. C. Jiang: 'Effects of alloy elements (Mg, Zn, Sn) on the microstructures and compression properties of high-volume-fraction TiC_x/Al composites', *Scr. Mater.*, **2010**, **63**, 1209–1211.
2. D. S. Zhou, F. Qiu and Q. C. Jiang: 'The nano-sized TiC particle reinforced Al–Cu matrix composite with superior tensile ductility', *Mater. Sci. Eng. A*, **2015**, **622**, 189–193.
3. S. L. Shu, J. B. Lu, F. Qiu, Q. Q. Xuan, and Q. C. Jiang: 'High volume fraction TiC_x/Al composites with good comprehensive performance fabricated by combustion synthesis and hot press consolidation', *Mater. Sci. Eng. A*, **2011**, **528**, 1931–1936.
4. I. Gotman, M. J. Koczak, and E. Shtessel: 'High volume fraction TiC_x/Al composites with good comprehensive performance fabricated by combustion synthesis and hot press consolidation', *Mater. Sci. Eng. A*, **1994**, **187**, 189–199.
5. Y. F. Yang and D. K. Mu: 'Rapid dehydrogenation of TiH₂ and its effect on formation mechanism of TiC during self-propagation high-temperature synthesis from TiH₂–C system', *Powder Technol.*, **2013**, **249**, 208–211.
6. Y. Choi and S. W. Rhee: 'Effect of aluminium addition on the combustion reaction of titanium and carbon to form TiC', *J. Mater. Sci.*, **1993**, **28**, 6669–6675.
7. M. Yaghoubi, A. Saidi and O. Torabi: 'In situ synthesis of Fe(Co)/TiC composite by self-propagating high temperature and mechanochemical methods', *Powder Metall.*, **2013**, **56**, (2), 164–169.
8. I. H. Song, D. K. Kim, Y. D. Hahn, and H. D. Kim: 'The effect of a dilution agent on the dipping exothermic reaction process for fabricating a high-volume TiC-reinforced aluminum composite', *Scr. Mater.*, **2003**, **48**, 413–418.
9. B. H. Li, Y. Liu, J. Li, H. Cao, and L. He: 'Fabrication of in situ TiB₂–TiC reinforced steel matrix composites by spark plasma sintering', *Powder Metall.*, **2011**, **54**, (3), 222–224.
10. Q. L. Lin, P. Shen, L. L. Yang, S. B. Jin, and Q. C. Jiang: 'Wetting of TiC by molten Al at 1123–1323 K', *Acta Mater.*, **2011**, **59**, 1898–1911.
11. Y. F. Yang and Q. C. Jiang: 'A simple route to fabricate TiC–TiB₂/Ni composite via thermal explosion reaction assisted with external pressure in air', *Mater. Chem. Phys.*, **2014**, **143**, 480–485.
12. Q. Q. Xuan, S. L. Shu, F. Qiu, S. B. Jin, and Q. C. Jiang: 'Different strain-rate dependent compressive properties and work-hardening capacities of 50 vol.-% TiC_x/Al and TiB₂/Al composites', *Mater. Sci. Eng. A*, **2012**, **538**, 335–339.
13. B. Yang, F. Wang, and J. S. Zhang: 'Microstructural characterization of in situ TiC/Al and TiC/Al–20Si–5Fe–3Cu–1Mg composites prepared by spray deposition', *Acta Mater.*, **2003**, **51**, 4977–4989.
14. Y. Birol: 'Grain refining efficiency of Al–Ti–C alloys', *J. Alloys Compd.*, **2006**, **422**, 128–131.
15. S. B. Jin, P. Shen, Q. L. Lin, L. Zhan, and Q. C. Jiang: 'Growth mechanism of TiC_x during self-propagating high-temperature synthesis in an Al–Ti–C system', *Cryst. Growth Des.*, **2010**, **10**, 1590–1597.
16. S. B. Jin, P. Shen, Y. J. Li, D. S. Zhou and Q. C. Jiang: 'Synthesis of spherical NbB_{2x} particles by controlling the stoichiometry', *Cryst. Eng. Commun.*, **2012**, **14**, 1925–1928.
17. N. Frumin, N. Frage, M. Polak, and M. P. Dariel: 'Wettability and phase formation in the TiC_x/Al system', *Scr. Mater.*, **1997**, **37**, 1263–1267.
18. V. A. Romanova, R. R. Balokhonov, and S. Schmauder: 'The influence of the reinforcing particle shape and interface strength on the fracture behavior of a metal matrix composite', *Acta Mater.*, **2009**, **57**, 97–107.
19. M. Kouzeli, L. Weber, C. Sanmarchi, and A. Mortensen: 'Influence of damage on the tensile behaviour of pure aluminium reinforced with ≥40 vol. pct alumina particles', *Acta Mater.*, **2001**, **49**, 3699–3709.
20. A. Fathy, F. Shehata, M. Abdelhameed, and M. Elmahdy: 'Compressive and wear resistance of nanometric alumina reinforced copper matrix composites', *Mater. Des.*, **2012**, **36**, 100–107.
21. P. K. Deshpande and R. Y. Lin: 'Wear resistance of WC particle reinforced copper matrix composites and the effect of porosity', *Mater. Sci. Eng. A*, **2006**, **418**, 137–145.